

LA-UR-18-25562 (Accepted Manuscript)

## Collective neutrino oscillations with the halo effect in single-angle approximation

Shalgar, Shashank M.

Provided by the author(s) and the Los Alamos National Laboratory (2019-06-26).

**To be published in:** Journal of Cosmology and Astroparticle Physics

**DOI to publisher's version:** 10.1088/1475-7516/2018/11/019

**Permalink to record:** <http://permalink.lanl.gov/object/view?what=info:lanl-repo/lareport/LA-UR-18-25562>

**Disclaimer:**

Los Alamos National Laboratory, an affirmative action/equal opportunity employer, is operated by Triad National Security, LLC for the National Nuclear Security Administration of U.S. Department of Energy under contract 89233218CNA000001. By approving this article, the publisher recognizes that the U.S. Government retains nonexclusive, royalty-free license to publish or reproduce the published form of this contribution, or to allow others to do so, for U.S. Government purposes. Los Alamos National Laboratory requests that the publisher identify this article as work performed under the auspices of the U.S. Department of Energy. Los Alamos National Laboratory strongly supports academic freedom and a researcher's right to publish; as an institution, however, the Laboratory does not endorse the viewpoint of a publication or guarantee its technical correctness.

# Collective neutrino oscillations with the halo effect in single-angle approximation

**Vincenzo Cirigliano, Mark Paris, Shashank Shalgar**

Theoretical Division, Los Alamos National Laboratory, Los Alamos, NM-87545 USA

E-mail: [cirigliano@lanl.gov](mailto:cirigliano@lanl.gov), [mparis@lanl.gov](mailto:mparis@lanl.gov), [shashankshalgar@gmail.com](mailto:shashankshalgar@gmail.com)

**Abstract.** We perform a self-consistent calculation of collective neutrino oscillations including the effect of back scattered neutrinos (Halo effect) in the ‘single-angle’ approximation, within a spherically symmetric supernova model. We find that due to the Halo effect the onset of flavor transformations is pushed to smaller radii, by a few kilometers. The celebrated phenomenon of the spectral split is found to be robust under the present inclusion of the Halo effect.

---

## Contents

<b>1</b>	<b>Introduction</b>	<b>1</b>
<b>2</b>	<b>Overview of flavor instability</b>	<b>3</b>
<b>3</b>	<b>Model set-up and formulation</b>	<b>4</b>
<b>4</b>	<b>Numerical results</b>	<b>7</b>
<b>5</b>	<b>Conclusion</b>	<b>8</b>
<b>6</b>	<b>Acknowledgments</b>	<b>10</b>

---

## 1 Introduction

The extreme astrophysical environment of a protoneutron star (PNS), formed within a few 10's of seconds after the collapse of a massive star (in the range  $\sim 8-50 M_{\odot}$ ), in the aftermath of a core-collapse supernova (CCSN), is largely characterized by the non-equilibrium evolution of its neutrino field. Indeed, about 99% of the gravitational energy released in the collapse is converted to neutrinos with almost  $\sim 10^{58}$  neutrinos emitted within the first few seconds; this number is about 20 orders of magnitude greater than the number of neutrinos emitted by the sun in one second. The reach and importance of neutrino flavor oscillation effects in astrophysical systems is difficult to overstate, as two familiar examples illustrate. Neutrino heating in CCSN, highly sensitive to neutrino flavor, may be pivotal in the determination of whether neutrinos are responsible for the revival of a stalled core-bounce shock[1–3]; the synthesis of  $r$ -process elements in extreme astrophysical environments is, too, expected to be sensitive to such oscillations[4].

Significant progress in the understanding of the evolution of the neutrino flavor field and the role of neutrino flavor oscillations, has been recently achieved[5–22]. Particularly interesting is the prospect of collective motion in flavor space, where the phase and frequency of neutrino flavor oscillations are independent of their momenta[7, 8, 23]. The effect is induced by coherent forward scattering, whose interaction strength is of bilinear form – the *sine qua non* of dense neutrino environments. It dictates, in high-flux neutrino environments, a non-perturbative setting that challenges both conventional analytical and computational approaches.

In spite of these achievements, a detailed description of the neutrino environment near the PNS in the aftermath of the CCSN remains incomplete. For example, the radius (or ‘epoch’), measured from the center of the PNS, at which flavor oscillations commence is only known in the simplest of models. This uncertain situation is largely a product of limitations imposed by both the complicated geometry of the PNS environment and the nonlinear nature of the non-equilibrium evolution of the neutrino flavor field, governed by the neutrino quantum kinetic equations[24–35] (QKE), which limits the use of analytical methods. We must, therefore, resort to numerical techniques.

Even then, given the complexity of the computational problem that is faced in the CCSN/PNS environment, limitations due to computational resource considerations force one

to reduce the full problem of the calculation of the neutrino flavor density matrix, parameterized generally by four spacetime coordinates and three momentum variables. The evolution of the neutrino flavor density matrix in this space of seven independent variables can be significantly reduced by assuming spherical symmetry.<sup>1</sup> The density matrix, under this assumption of spherical symmetry, is then a function only of the zenith angle of the momentum  $\vec{p}$ , the energy  $E$  (or  $|\vec{p}|$ ), and the distance  $r$  from the center of the PNS. Realistic scenarios at radii far from the PNS are considerably more complicated than the simple, spherically symmetric picture allows. While the validity of assuming a simplified geometry remains to be determined [19, 21, 22, 37, 39], it is hoped that by considering this simplified setup, insight may be gained into the nature of neutrino flavor transformation in the complex astrophysical environment in the vicinity of the PNS.

The pioneering study of Cherry *et al.* [40] explored the consequences of perturbing the neutrino “bulb” model, wherein neutrinos are assumed to trace straight-line trajectories for radii  $r > R_\nu$ , defining the “neutrinosphere.” They realized that even a small number (about 1 part in  $10^3$ ) of neutrinos that suffer direction-changing scatterings, residing in a “halo” above the PNS, have the potential to alter the radial neutrino flavor field evolution significantly. This is due to the PNS geometry, the form of the forward-scattering neutrino-neutrino ( $\nu\nu$ ) self-interaction, and the non-linearity of the problem. The magnitude of contributions to the *diagonal* elements of the  $\nu\nu$  self-interaction Hamiltonian  $H_{\nu\nu}$  from the bulb  $|H_{\nu\nu}^{\text{bulb}}|$  and halo  $|H_{\nu\nu}^{\text{halo}}|$  contributions were investigated in Ref. [40]; phase differences induced by the medium during neutrino propagation were neglected and contributions to  $|H_{\nu\nu}^{\text{halo}}|$  were assumed to arise from neutrinos scattered by a single direction-changing scattering. The tantalizing results of their study suggest the possibility of a significant role for the halo in determining the evolution of the PNS neutrino flavor field with an enhancement of  $|H_{\nu\nu}^{\text{halo}}|/|H_{\nu\nu}^{\text{bulb}}|$  by a factor of up to 10 at distances 1000–2000 km from the PNS. The neutrino self-interaction falls off as the forth power of the radius while the collision term, which is proportional to the matter density falls off approximately like the third power of the radius, which increases the relative strength of the Halo Hamiltonian with respect to the bulb Hamiltonian. Given this linear increase in the ratio of  $|H_{\nu\nu}^{\text{halo}}|/|H_{\nu\nu}^{\text{bulb}}|$ , we take as our departure for the current study the question posed by Ref. [40] of whether scattered-halo feedback effects push flavor oscillations to smaller radii. We find, in fact, that such a hastening of the flavor transformation is expected but likely too small to observe.

In the present work, we investigate the effect of going beyond the approximations of Ref. [40]. Using a collision term rooted in the QKE [35], we compute the effect of neutrino back-scattering, the halo effect, through an iterative, and therefore self-consistent, approach within the ‘single-angle’ approximation. A broader theme we touch upon is the robustness of the spectral splits seen in the simulations of the neutrino flavor oscillations in the interior of a core-collapse supernova. We find that the spectral split is seen in the final electron neutrino spectrum in the single-angle approximation even upon the inclusion of the backscattered neutrinos.

Relaxing the assumption that those neutrinos which back-scatter from nuclei do not contribute to the neutrino-neutrino self-interaction increases the computational complexity of the problem relative to that of the bulb model. We have implemented the effect of neutrino back-scattering in the single-angle approximation, using a simplified collision term derived from the full expressions in Ref. [35]. At each radius there is a finite probability of neutrino

---

<sup>1</sup>We are, for the present work, ignoring the fact that inhomogeneity and anisotropy [21, 22, 36–38] is unstable with respect to seed fluctuations due to the nonlinear nature of the neutrino QKE.

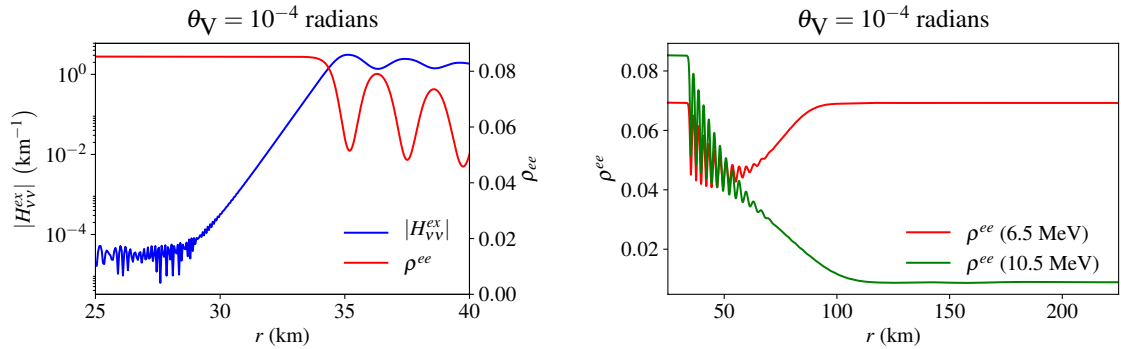


**Figure 1.** Left panel: The logarithm of the off-diagonal term of the  $\nu\nu$  Hamiltonian,  $H_{\nu\nu}^{ex}$  (blue curve; color online) and the electron neutrino flux,  $\rho^{ee}$  (red curve; color online) at an energy of 8.5 MeV. The neutrino flavor instability, signaled by the variation of the  $H_{\nu\nu}^{ex}$  with radius, commences at radii  $\sim 29$  km. At larger radii, beyond 33 km, when the off-diagonal term of Hamiltonian attains its maximum and no longer varies with radius, we observe the onset of neutrino oscillations. Right panel: We plot electron neutrino flux, in arbitrary inverse-energy units, for two representative energies, below and above the split energy. Above the split energy the electron neutrino flux returns to its initial value.

back-scattering and we take into account the effect of the back-scattered neutrinos on the neutrino flavor evolution. While the neutrino-bulb model is an initial value problem, including the back-scattered neutrinos transforms it into a boundary value problem.

In the following section, we review the essential physics of neutrino flavor evolution in the bulb model. We detail, in Sec. 3, the present halo model formulation and solution method. Finally, we discuss the results (Sec. 4) of these calculations and conclude in Sec. 5 with a summary of the main results.

## 2 Overview of flavor instability

We review the neutrino flavor oscillations in the context of the bulb model, the simplest, perhaps, of models that attempt to capture coherent oscillation effects in the PNS environment. The bulb model assumes a spherical and sharp transition at  $R_\nu$  from trapped- to free-neutrinos. This approximation should capture gross features in the complicated environment, as long as the neutrino flavor instability has an onset at a relatively large radius compared to  $R_\nu$ . The bulb model takes into account the effects of  $\nu\nu$  self-interaction but neglects the effect of neutrinos back-scattered by matter in the PNS environment. This discussion is intended to provide an overview of the essential physics of neutrino flavor instability, which remains largely relevant in the present calculation of the onset of flavor instability. We work with two effective neutrino flavors labeled  $e$  and  $x$  and describe neutrinos by a  $2 \times 2$  density matrix  $\rho_{\alpha\beta}$ , with  $\alpha, \beta \in \{e, x\}$ . We assume a value of  $R_\nu = 11$  km for this work.

We consider the equations of motion of the neutrino density matrix  $\rho$  in the presence of three contributions to the evolution operator  $H$ : the vacuum contribution  $H_0$ , the matter-effect term  $H_m$ , and the neutrino self-interaction term  $H_{\nu\nu}$ . The Hamiltonian  $H$  can be represented as traceless  $2 \times 2$  matrix and the amplitude of the neutrino flavor transformation is determined by the ratio of the off-diagonal element to the diagonal element.

In the neutrino bulb-model, the strength of the neutrino self-interaction potential is very large near the proto-neutron star ( $H \sim H_{\nu\nu}$  is diagonal) and there is no flavor instability as a result<sup>2</sup>. The size of the off-diagonal terms of  $H$ , in this case, is determined by the vacuum mixing angle as well as the matter density. As the radial distance increases, the self-interaction decreases until neutrino flavor instability is reached and the off-diagonal terms of the Hamiltonian grow exponentially. The onset of instability is controlled by the relative size of the vacuum Hamiltonian  $H_0$  and the diagonal components of  $H_{\nu\nu}$ . Similarly, the exponential growth is controlled by the diagonal components of  $H_{\nu\nu}$ , as can be seen from a linear stability analysis [41].

Exponential growth of the off-diagonal element of  $H$ , driven by the non-linear neutrino self-interaction  $H_{\nu\nu}$ , eventually triggers the onset of neutrino flavor transformation as seen in Fig.1 at radii  $\gtrsim 35$  km. As the distance from the proto-neutron star increases, the neutrino flavor reaches a steady state configuration, characterized by a spectral split ( $\nu_e$  and  $\nu_x$  spectra above a certain energy  $E_c$  get swapped). On the right hand side panel of Fig. 1 we can see this phenomenon in our numerical simulations. For a representative energy lower than  $E_c$  the  $\rho_{ee}$  component of the density matrix returns to the initial value, whereas for a representative energy above  $E_c$  the flux approaches the initial  $x$  flux (not shown in the figure). To summarize, there are two regions, near the proto-neutron star and away from the proto-neutron star, where the flavor does not evolve significantly, but for different reasons.

As we will show later the magnitude of modification to the Hamiltonian due to the Halo effect is of consequence only in the region of significant flavor transformation. In the model we consider, the Halo effect does not lead to additional exponential growth due to its inclusion. We find that the inclusion of the Halo effect does not change the region of instability or the exponential growth rate of the off-diagonal term in the neutrino-bulb model with single-angle approximation.

This occurs because the Halo neutrinos affect the diagonal entries of  $H_{\nu\nu}$ , which control both the onset of instabilities and their growth rate, only at the percent level for radii of interest. However, we find that at small radii the off-diagonal entries of  $H_{\nu\nu}$  are significantly modified due to the Halo effect. This in turns can change the radius at which the off-diagonal terms of the Hamiltonian become comparable to the diagonal terms and start to affect the neutrino flavor content. We demonstrate this effect using numerical simulations of the equations of motion given in the following section.

### 3 Model set-up and formulation

In order to study the Halo effect we consider a simple spherically symmetric model. The neutrino sphere, of radius  $R_\nu$ , is assumed to emit neutrinos with only one emission angle. At each point during its propagation there is a finite probability for the neutrino to scatter backwards along the same path, but in the opposite direction. For simplicity we work in two flavor approximation with a pinched thermal spectrum.

Our objective is to find a steady state solution for this problem, where the outgoing neutrinos experience self-interaction due to other outgoing neutrino and the back-scattered neutrinos. The reflected neutrinos also experience potential due to other reflected neutrino

---

<sup>2</sup>The assumption of flavor stability at large neutrino flux is not necessarily valid when the assumptions of neutrino bulb-model are relaxed. These assumptions include spherical symmetry and a sharp transition to free streaming of neutrinos of all flavors at a particular radius.

and outgoing neutrinos. In this section, we describe the equations of the motion we use for the system, namely the appropriate QKEs.

As discussed earlier, assuming spherical symmetry the  $n_f \times n_f$  density matrices ( $n_f$  is the number of flavors) depend on the neutrino energy  $E$ , the angle  $\vartheta$  of the neutrino momentum with respect to the radial direction, and the radial coordinate  $r$ , i.e.  $\rho = \rho(E, \cos \vartheta, r)$ . In the bulb model, which ignores direction-changing scattering, at a given radius  $r$  the angle  $\vartheta$  is related to the emission angle  $\vartheta_E$  by

$$\cos \vartheta = \sqrt{1 - \frac{R_\nu^2}{r^2} (1 - \cos^2 \vartheta_E)}. \quad (3.1)$$

In the single-angle approximation we use in this paper, only one emission angle is considered, which we call  $\vartheta_0$ , and therefore at a given radius  $r$  only a single angle  $\vartheta(r, \vartheta_0)$  is allowed, defining a cone around the radial direction. We *define* the single-angle approximation in presence of direction-changing collisions by enforcing that the scattered neutrinos at a given radius  $r$  are restricted to the cone defined by  $\vartheta(r, \vartheta_0)$ . A neutrino scattered in the forward hemisphere is characterized by  $\vartheta(r, \vartheta_0)$ , while a neutrino scattered in the backward hemisphere is characterized by  $\pi - \vartheta(r, \vartheta_0)$ . We use the following simplified notation:  $\rho(E, \cos \vartheta, r) \equiv \rho^\uparrow(E, r)$  and  $\bar{\rho}(E, \cos \vartheta, r) \equiv \bar{\rho}^\uparrow(E, r)$  correspond to outgoing neutrinos and anti-neutrinos, while  $\rho(E, -\cos \vartheta, r) \equiv \rho^\downarrow(E, r)$  and  $\bar{\rho}(E, -\cos \vartheta, r) \equiv \bar{\rho}^\downarrow(E, r)$  correspond to back-scattered (anti)neutrinos.

The QKEs governing the evolution of these density matrices are given by,

$$\frac{\partial \rho^\uparrow(E, r)}{\partial r} = -\frac{i}{\cos \vartheta} [H^\uparrow, \rho^\uparrow(E, r)] - \mathcal{C}^{\text{loss}\uparrow} \rho^\uparrow(E, r) + \mathcal{C}^{\text{gain}\uparrow} \rho^\downarrow(E, r) \quad (3.2a)$$

$$\frac{\partial \bar{\rho}^\uparrow(E, r)}{\partial r} = -\frac{i}{\cos \vartheta} [\bar{H}^\uparrow, \bar{\rho}^\uparrow(E, r)] - \mathcal{C}^{\text{loss}\uparrow} \bar{\rho}^\uparrow(E, r) + \mathcal{C}^{\text{gain}\uparrow} \bar{\rho}^\downarrow(E, r) \quad (3.2b)$$

$$\frac{\partial \rho^\downarrow(E, r)}{\partial r} = -\frac{i}{\cos \vartheta} [H^\downarrow, \rho^\downarrow(E, r)] - \mathcal{C}^{\text{loss}\downarrow} \rho^\downarrow(E, r) + \mathcal{C}^{\text{gain}\downarrow} \rho^\uparrow(E, r) \quad (3.2c)$$

$$\frac{\partial \bar{\rho}^\downarrow(E, r)}{\partial r} = -\frac{i}{\cos \vartheta} [\bar{H}^\downarrow, \bar{\rho}^\downarrow(E, r)] - \mathcal{C}^{\text{loss}\downarrow} \bar{\rho}^\downarrow(E, r) + \mathcal{C}^{\text{gain}\downarrow} \bar{\rho}^\uparrow(E, r). \quad (3.2d)$$

Our aim is to find a solution to these equations subject to the boundary conditions

$$\rho^{\uparrow ee}(E, R_\nu) = \kappa^e f^e(E) \quad (3.3)$$

$$\rho^{\uparrow xx}(E, R_\nu) = \kappa^x f^x(E) \quad (3.4)$$

$$\bar{\rho}^{\uparrow ee}(E, R_\nu) = \kappa^{\bar{e}} f^{\bar{e}}(E) \quad (3.5)$$

$$\bar{\rho}^{\uparrow xx}(E, R_\nu) = \kappa^x f^x(E) \quad (3.6)$$

$$\rho^{\uparrow ex}(E, R_\nu) = 0 \quad (3.7)$$

$$\bar{\rho}^{\uparrow ex}(E, R_\nu) = 0 \quad (3.8)$$

$$\rho^\downarrow(E, r^{\text{max}}) = 0 \quad (3.9)$$

$$\bar{\rho}^\downarrow(E, r^{\text{max}}) = 0, \quad (3.10)$$

where  $r^{\text{max}} \rightarrow \infty$ . Here  $f^i$  are the initial thermal spectra for various flavors at the neutrino sphere given by the Fermi-Dirac distribution,

$$f^i(E) = \frac{E^2}{1 + \exp(E/T_i - \eta_i)}. \quad (3.11)$$

The normalization constants,

$$\kappa^i = \frac{1}{\int_0^\infty f^i(E) dE} \frac{j_i}{j_e}, \quad (3.12)$$

are used to normalize the thermal spectra, which sets the scale for  $\rho_{ee}$  in Figs. 1-5. Here,  $j_i$  is the flux of the  $i^{\text{th}}$  flavor of the neutrinos which is equal to the ratio of luminosity and the average energy,  $\frac{L_i}{\langle E_i \rangle}$ . The flux of neutrinos, which is the coefficient of the self-interaction Hamiltonian, is adjusted to have luminosity of  $10^{51}$  ergs/sec for all flavors. We also assume that the degeneracy factors  $\eta_i = \mu_i/T$  are the same for all flavors and are equal to 3.0. We use temperature values of  $T_e = 2.76$  MeV,  $T_{\bar{e}} = 4.01$  MeV and  $T_x = T_{\bar{x}} = 6.26$  MeV [42].

We now describe in detail each term on the RHS of eqs. (3.2). First, note that the factor of  $1/\cos\vartheta$  on the right hand side of eq. (3.2a),(3.2b),(3.2c),(3.2d) is a geometrical factor to convert path length traversed by the neutrino to radius.

Next, the four Hamiltonians determining the coherent evolution of density matrices are given by,

$$H^{\uparrow(\downarrow)} = H_0 + H_m + H_{\nu\nu}^{\uparrow(\downarrow)} \quad (3.13)$$

$$\bar{H}^{\uparrow(\downarrow)} = -H_0 + H_m + H_{\nu\nu}^{\uparrow(\downarrow)} \quad (3.14)$$

where,

$$H_0 = \frac{1}{2} \begin{pmatrix} -\omega \cos 2\theta_V & \omega \sin 2\theta_V \\ \omega \sin 2\theta_V & \omega \cos 2\theta_V \end{pmatrix} \quad (3.15)$$

$$H_m = \begin{pmatrix} \sqrt{2}G_F n_e & 0 \\ 0 & 0 \end{pmatrix} \quad (3.16)$$

$$H_{\nu\nu}^{\uparrow} = \mu \int_0^\infty dE' \left( \rho^{\uparrow}(E', r) - \bar{\rho}^{\uparrow}(E', r) \right) (1 - \cos^2 \vartheta) \\ + \mu \int_0^\infty dE' \left( \rho^{\downarrow}(E', r) - \bar{\rho}^{\downarrow}(E', r) \right) (1 + \cos^2 \vartheta), \quad (3.17)$$

$$H_{\nu\nu}^{\downarrow} = \mu \int_0^\infty dE' \left( \rho^{\downarrow}(E', r) - \bar{\rho}^{\downarrow}(E', r) \right) (1 - \cos^2 \vartheta) \\ + \mu \int_0^\infty dE' \left( \rho^{\uparrow}(E', r) - \bar{\rho}^{\uparrow}(E', r) \right) (1 + \cos^2 \vartheta). \quad (3.18)$$

$\omega$  is the vacuum oscillation frequency which is equal to  $\frac{\Delta m^2}{2E}$ . The coefficient of self-interaction potential,  $\mu$ , is adjusted so that the total neutrino luminosity for all the flavors is  $10^{51}$  ergs/sec, and takes the form  $\mu(r) = \sqrt{2}G_F n_\nu(r)$  with  $n_\nu(r) = \frac{L_{\nu e}}{\langle E_{\nu e} \rangle 2\pi r^2} \frac{\cos\vartheta_0}{\cos\vartheta}$ .

Finally,  $\mathcal{C}^{\uparrow}(E)$  and  $\mathcal{C}^{\downarrow}(E)$  are the collision terms for outgoing and incoming neutrinos beams. There are two terms for each bin, corresponding to loss and gain (i.e. scattering out of or into the given bin), as indicated by the superscript. The form of the collision term used in eqs. (3.2a) can be derived from the general results of Ref. [35] for neutrino-nucleon (or neutrino-nucleus) scattering, under the following assumptions: (i) neglecting Pauli blocking for both neutrinos and targets: this corresponds to non-degenerate species; (ii) treating targets as very heavy and non-relativistic ( $M \gg T$ ): this implies that collisions do not change the neutrino energy, which is an excellent approximation for the halo problem of neutrino scattering off nuclei; (iii) performing the angular integrals consistently with the

single-angle approximation: this implies that a neutrino of momentum  $(|\vec{k}|, \cos \vartheta)$  can only scatter into a final state with momentum  $(|\vec{k}|, \pm \cos \vartheta)$  (forward or backwards cones).

The individual terms have to satisfy  $\mathcal{C}^{\text{loss}\uparrow} = \mathcal{C}^{\text{gain}\downarrow}$  and  $\mathcal{C}^{\text{loss}\downarrow} = \mathcal{C}^{\text{gain}\uparrow}$  to be consistent with the principle of detailed balance. Explicit calculation as sketched above reveals that  $\mathcal{C}^{\text{loss}\uparrow} = \mathcal{C}^{\text{gain}\uparrow}$ , namely all entries are equal. The explicit calculation also shows that  $\mathcal{C}^{\text{loss}\uparrow} = n_T G_F^2 E^2 C_W / \pi$ , where  $n_T$  is the number density of targets,  $G_F$  is the Fermi constant, and  $C_W$  is a coupling of  $O(1)$  proportional to the weak charge of the target.

An order-of-magnitude estimate of  $\mathcal{C}^{\text{loss}\uparrow}$  can be obtained as follows. First, note that for neutrino-nucleon scattering the collision term goes like  $\sim G_F^2 E^2 n_e$  while the matter potential goes like  $\sim G_F n_e$ . The collision term is thus related to the matter potential by a factor of about  $\sim G_F \langle E^2 \rangle \approx 10^{-9}$ . Notice that by taking the average of the energy-squared we have ignored the energy dependence which does not affect the results significantly. Since the cross section can be enhanced by two or three orders of magnitude for scattering off nuclei (through the coherence factor of  $A^2$ ), it is quite reasonable to estimate the maximum effect of the collision term by using  $\mathcal{C} \sim 10^{-6} \sqrt{2} G_F n_e$ . We use a matter profile that falls off with the third power of the radius with an entropy per baryon of 140. Choosing numerical parameters this way corresponds to about a percent of the neutrinos experiencing direction-changing scatterings, compared to an estimate of 0.1 percent mentioned in [40]. We have purposely used a collision term which is almost an order of magnitude larger.

## 4 Numerical results

It should be noted that the boundary conditions for eq. (3.3), (3.4), (3.5), (3.6) and eq. (3.7), (3.10) are at two different radii. This makes the problem unsolvable by a direct application of the forward-difference method. We employ an iterative forward-difference method to solve this boundary value problem.

In this section we describe the methodology we use and the numerical results we obtain. For the zeroth iteration we solve the equations of motion and evolve  $\rho$  and  $\bar{\rho}$  from  $r^{\text{min}}$  to  $r^{\text{max}}$ , ignoring the Halo effect ( $\mathcal{C}_{\text{loss}} = \mathcal{C}_{\text{gain}} = 0$ ). Then using eq. (3.2c), (3.2d) we evolve  $\rho^\downarrow$  and  $\bar{\rho}^\downarrow$  from  $r^{\text{max}}$  to  $r^{\text{min}}$  using  $\rho$  and  $\bar{\rho}$  from the previous step. Now that we have an initial estimate for  $\rho^\downarrow$  and  $\bar{\rho}^\downarrow$  we use those to solve eq. (3.2a) and (3.2b) and proceed with the next iterative steps. For our computation we use  $r_{\text{min}} = 15$  km and  $r_{\text{max}} = 515$  km.

For all but the first iteration in the radially outward direction, values of  $\rho^\downarrow$  are required for calculation of  $\rho^\uparrow$  and vice-versa. The values required are not on a fixed grid but are determined by adaptive Runge-Kutta. After each calculation of  $\rho^\uparrow$ , we store the radial dependence of each energy bin as a spline curve for use in the following calculation of  $\rho^\downarrow$  and then store those density matrices as spline curves for use in the following calculation of  $\rho^\uparrow$ . We use 80 energy bins in the range of 0 to 80 MeV and there are 8 components of density matrix for each energy bin. We thus store 640 spline curves in memory at all times during the evolution of the code. We use the publicly available GNU Scientific Library (GSL) to perform this task [43].

On the left panels of Figs. 2, 3 and 4 we plot  $\rho_{ee}$  for the 10th energy bin corresponding to the energy of 8.5 MeV for 15 iterations in the region of neutrino flavor onset. On the right panels, we plot the off-diagonal term of the self-interaction Hamiltonian for 15 different iterations and the off-diagonal for the contribution due to the Halo effect alone. Figs. 2, 3 and 4 correspond to different values for the vacuum mixing angle, namely  $\theta_V = 10^{-4}, 10^{-3}, 10^{-2}$ . It can be clearly seen that for small values of the mixing angle, when initially the contribu-

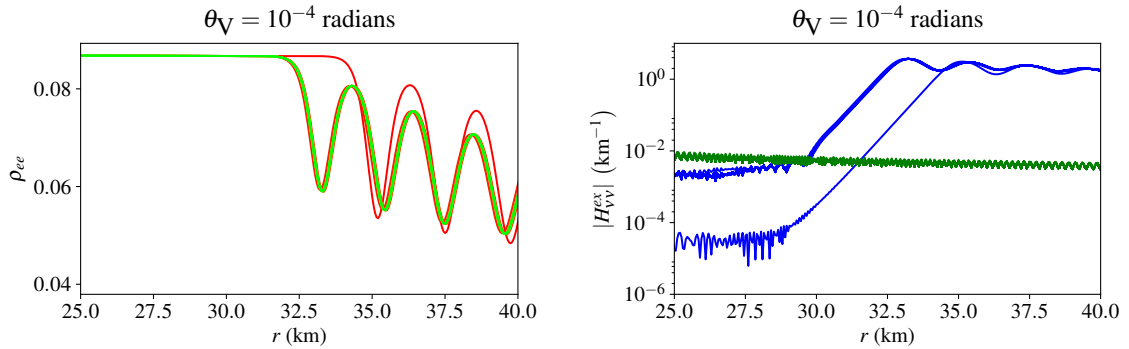


**Figure 2.** The onset of neutrino oscillations on the left for energy bin of 8.5 MeV. The left plot has 15 iterations which gradually go from red to green, however only two plots are visible as the effect of Halo converges after the second iteration. On the right we plot the off-diagonal term of the Hamiltonian on log scale in blue for 15 iterations. The blue one which starts off with small magnitude is the first iteration. On the right hand side we also plot the off-diagonal term of the Hamiltonian due to the Halo term only in green. The vacuum mixing angle is set to  $10^{-4}$  radians.

tion of the Halo effect is large compared to the off-diagonal term without the Halo effect, the convergence is swift and happens mostly by the second iteration. On the other hand, when the contribution of the Halo term to the off-diagonal term is comparable to the off-diagonal term without the Halo effect, the convergence requires a few iterations, but the overall effect remains small.

It should be noted that the off-diagonal term of  $H_{\nu\nu}$  without the Halo effect is proportional to  $(1 - \cos^2 \vartheta)$  which in turn depends on  $\vartheta_0$ , the emission angle which is fixed in our case to  $5^\circ$ . For larger values of  $\vartheta_0$ , the off-diagonal term is larger to begin with and the Halo's impact is less pronounced. For smaller emission angles the relative effect of the Halo is larger but the flux from small emission angle is suppressed due to the geometric factor, eq. 3.1.

From the right panels of Figs. 2, 3 and 4 we can see that the back-scattering increases the small  $r$  value of the off-diagonal element of the self-interaction Hamiltonian  $H_{\nu\nu}$ . The radius at which the exponential growth of the off-diagonal element begins and the value of the exponent remain unchanged, and the two effects together lead to an onset of flavor transformation at a smaller radius, reduced by a few kilometers with respect to the standard bulb model.

## 5 Conclusion

In this paper we have formulated the problem of collective neutrino oscillations with the Halo effect in terms of appropriate QKEs with simplified collision terms, and have adapted those to the single-angle approximation. We have then obtained a self-consistent solution for the resulting boundary value problem using an iterative method. Our main findings can be summarized as follows:

- Halo effects modify the size of the various components of the Hamiltonian  $H_{\nu\nu}$  consistently with the expectations of Ref. [40]. In particular, the modification can be dramatic at large radii. At this large distance where the neutrino flavor field has stopped evolving, the Halo potential is large compared to the self-interaction potential, but it does

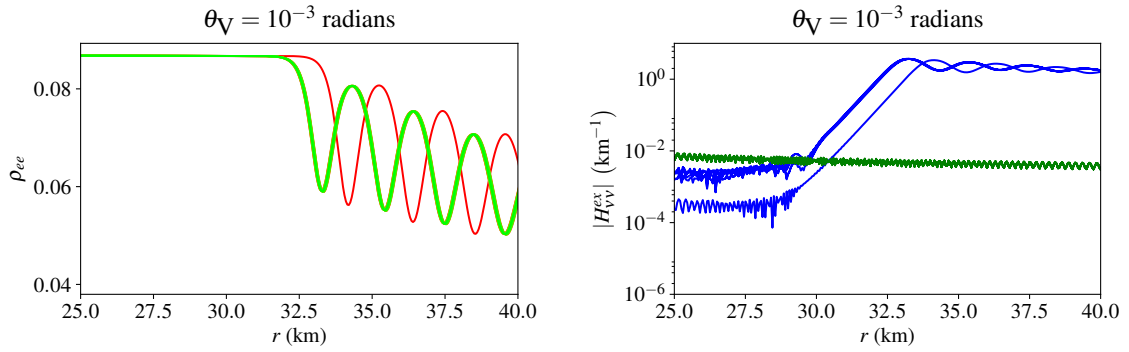


**Figure 3.** Same as Fig. 2 but for vacuum mixing angle set to  $10^{-3}$  radians.

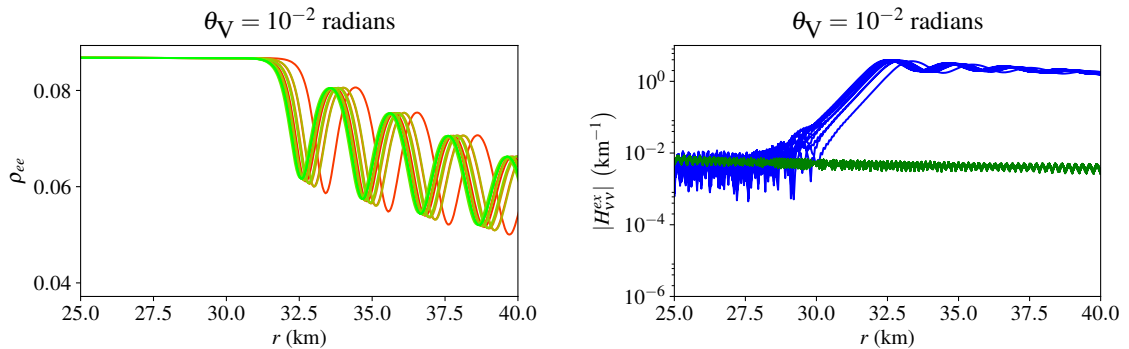


**Figure 4.** Same as Fig. 2 but for vacuum mixing angle set to  $10^{-2}$  radians.

not trigger additional flavor instabilities. On the other hand the influence of the Halo potential is more important in the region near the onset of neutrino flavor instability.

- At the onset of neutrino flavor instability, the main impact of the Halo is to increase the value of the off-diagonal element of the self-interaction Hamiltonian  $H_{\nu\nu}$  by about two orders of magnitude (for small vacuum mixing angle). On the other hand, at these radii the Halo affects the diagonal elements of  $H_{\nu\nu}$  at the sub-percent level, and hence it has little impact on the radius at which the instability arises and on the rate of exponential growth of the off-diagonal elements of  $H_{\nu\nu}$ . These features together lead to an onset of flavor transformation at a smaller radius, reduced by a few kilometers, as illustrated in Figs. 2, 3 and 4.
- An important question that has been repeatedly raised in the literature regarding the collective neutrino oscillations in the vicinity of core-collapse supernova is about the robustness of the split. At least in the case of single angle approximation, the feature of split seems to survive the inclusion of the Halo effect, as illustrated in Fig. 5.
- We find that in the simplest of the supernova models, assuming spherical symmetry, the Halo has an effect which is equivalent to increasing the effective mixing angle – a conclusion we expect would carry on to the multi-angle calculations. The overall

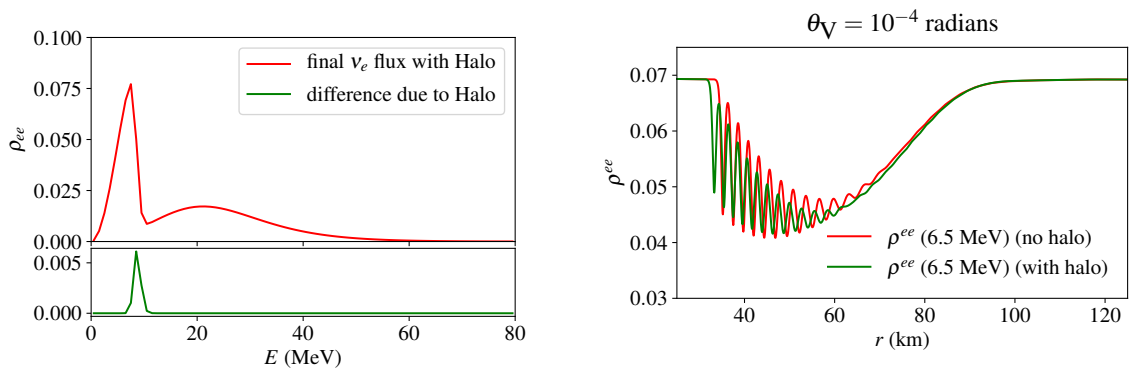


**Figure 5.** Final electron neutrino flux with the Halo effect. In the left panel we can see that the ‘spectral split’ feature; the discontinuity in the flux is preserved when Halo effect is included. For comparison we also plot the difference between the results with no Halo effect and the one with Halo effect. The Halo effect has a very limited influence on the shape of the final neutrino spectra. In the right hand side panel we plot the flux as a function of radius for a single energy. We can see that although the radius of flavor onset is changed by the inclusion of the Halo effect, the final flux remains unchanged.

impact of the Halo effect is thus expected to be very limited in a spherical model of neutrino emission from a supernova.

Looking ahead, our work can be extended and generalized in several directions, with different degree of technical difficulty. First, let us note that the matter profile we use, and hence the radial dependence of the strength of the Halo effect, is smooth. However, in the interior of a supernova environment, there can be sharp changes in matter density and the nuclear composition. The effect of an abrupt change in the strength of the collisions certainly warrants further investigation. Finally, while it seems quite plausible that the qualitative effects of the Halo found in this single angle calculation survive in a realistic model, we think that future work should be devoted to exploring a multi-angle scheme.

## 6 Acknowledgments

We are extremely grateful to George Fuller and Baha Balantekin for many engaging discussions. SS would like to thank the N3AS collaboration for the hospitality and opportunity to discuss this work with several colleagues during the first annual N3AS collaboration meeting in University of California, San Diego. Research presented in this article was supported by the Laboratory Directed Research and Development program of Los Alamos National Laboratory under Project #20170430ER.

## References

- [1] H. A. Bethe and J. R. Wilson, *Revival of a stalled supernova shock by neutrino heating*, *Astrophys. J.* **295** (1985) 14–23.
- [2] T. D. Brandt, A. Burrows, C. D. Ott and E. Livne, *Results From Core-Collapse Simulations with Multi-Dimensional, Multi-Angle Neutrino Transport*, *Astrophys. J.* **728** (2011) 8, [[1009.4654](#)].

- [3] H.-T. Janka, K. Langanke, A. Marek, G. Martinez-Pinedo and B. Mueller, *Theory of Core-Collapse Supernovae*, *Phys. Rept.* **442** (2007) 38–74, [[astro-ph/0612072](#)].
- [4] H. Duan, A. Friedland, G. C. McLaughlin and R. Surman, *The influence of collective neutrino oscillations on a supernova r-process*, *J. Phys.* **G38** (2011) 035201, [[1012.0532](#)].
- [5] J. T. Pantaleone, *Neutrino flavor evolution near a supernova’s core*, *Phys. Lett.* **B342** (1995) 250–256, [[astro-ph/9405008](#)].
- [6] H. Duan, G. M. Fuller and Y.-Z. Qian, *Collective neutrino flavor transformation in supernovae*, *Phys. Rev.* **D74** (2006) 123004, [[astro-ph/0511275](#)].
- [7] H. Duan, G. M. Fuller, J. Carlson and Y.-Z. Qian, *Simulation of Coherent Non-Linear Neutrino Flavor Transformation in the Supernova Environment. 1. Correlated Neutrino Trajectories*, *Phys. Rev.* **D74** (2006) 105014, [[astro-ph/0606616](#)].
- [8] H. Duan, G. M. Fuller, J. Carlson and Y.-Z. Qian, *Coherent Development of Neutrino Flavor in the Supernova Environment*, *Phys. Rev. Lett.* **97** (2006) 241101, [[astro-ph/0608050](#)].
- [9] H. Duan, G. M. Fuller, J. Carlson and Y.-Z. Qian, *Analysis of Collective Neutrino Flavor Transformation in Supernovae*, *Phys. Rev.* **D75** (2007) 125005, [[astro-ph/0703776](#)].
- [10] H. Duan, G. M. Fuller and Y.-Z. Qian, *Stepwise spectral swapping with three neutrino flavors*, *Phys. Rev.* **D77** (2008) 085016, [[0801.1363](#)].
- [11] G. G. Raffelt and A. Yu. Smirnov, *Adiabaticity and spectral splits in collective neutrino transformations*, *Phys. Rev.* **D76** (2007) 125008, [[0709.4641](#)].
- [12] A. Esteban-Pretel, S. Pastor, R. Tomas, G. G. Raffelt and G. Sigl, *Multi-angle effects in collective supernova neutrino oscillations*, *J. Phys. Conf. Ser.* **120** (2008) 052021, [[0712.2176](#)].
- [13] A. Esteban-Pretel, A. Mirizzi, S. Pastor, R. Tomas, G. G. Raffelt, P. D. Serpico et al., *Role of dense matter in collective supernova neutrino transformations*, *Phys. Rev.* **D78** (2008) 085012, [[0807.0659](#)].
- [14] G. G. Raffelt, *Self-induced parametric resonance in collective neutrino oscillations*, *Phys. Rev.* **D78** (2008) 125015, [[0810.1407](#)].
- [15] B. Dasgupta, G. G. Raffelt and I. Tamborra, *Triggering collective oscillations by three-flavor effects*, *Phys. Rev.* **D81** (2010) 073004, [[1001.5396](#)].
- [16] A. Malkus, A. Friedland and G. C. McLaughlin, *Matter-Neutrino Resonance Above Merging Compact Objects*, **1403.5797**.
- [17] Y.-L. Zhu, A. Perego and G. C. McLaughlin, *Matter Neutrino Resonance Transitions above a Neutron Star Merger Remnant*, *Phys. Rev.* **D94** (2016) 105006, [[1607.04671](#)].
- [18] M.-R. Wu, H. Duan and Y.-Z. Qian, *Physics of neutrino flavor transformation through matter-neutrino resonances*, *Phys. Lett.* **B752** (2016) 89–94, [[1509.08975](#)].
- [19] G. Raffelt, S. Sarikas and D. de Sousa Seixas, *Axial Symmetry Breaking in Self-Induced Flavor Conversion of Supernova Neutrino Fluxes*, *Phys. Rev. Lett.* **111** (2013) 091101, [[1305.7140](#)].
- [20] S. Chakraborty and A. Mirizzi, *Multi-azimuthal-angle instability for different supernova neutrino fluxes*, *Phys. Rev.* **D90** (2014) 033004, [[1308.5255](#)].
- [21] H. Duan and S. Shalgar, *Flavor instabilities in the neutrino line model*, *Phys. Lett.* **B747** (2015) 139–143, [[1412.7097](#)].
- [22] S. Abbar, H. Duan and S. Shalgar, *Flavor instabilities in the multiangle neutrino line model*, *Phys. Rev.* **D92** (2015) 065019, [[1507.08992](#)].
- [23] H. Duan, G. M. Fuller, J. Carlson and Y.-Z. Qian, *Neutrino Mass Hierarchy and Stepwise Spectral Swapping of Supernova Neutrino Flavors*, *Phys. Rev. Lett.* **99** (2007) 241802, [[0707.0290](#)].

- [24] G. Sigl and G. Raffelt, *General kinetic description of relativistic mixed neutrinos*, *Nucl. Phys.* **B406** (1993) 423–451.
- [25] G. Raffelt, G. Sigl and L. Stodolsky, *NonAbelian Boltzmann equation for mixing and decoherence*, *Phys. Rev. Lett.* **70** (1993) 2363–2366, [[hep-ph/9209276](#)].
- [26] B. H. J. McKellar and M. J. Thomson, *Oscillating doublet neutrinos in the early universe*, *Phys. Rev.* **D49** (1994) 2710–2728.
- [27] K. Enqvist, K. Kainulainen and J. Maalampi, *Refraction and Oscillations of Neutrinos in the Early Universe*, *Nucl. Phys.* **B349** (1991) 754–790.
- [28] P. Strack and A. Burrows, *Generalized Boltzmann formalism for oscillating neutrinos*, *Phys. Rev.* **D71** (2005) 093004, [[hep-ph/0504035](#)].
- [29] C. Volpe, D. VAAdnAdn and C. Espinoza, *Extended evolution equations for neutrino propagation in astrophysical and cosmological environments*, *Phys. Rev.* **D87** (2013) 113010, [[1302.2374](#)].
- [30] C. Volpe, *Neutrino Quantum Kinetic Equations*, *Int. J. Mod. Phys.* **E24** (2015) 1541009, [[1506.06222](#)].
- [31] A. Vlasenko, G. M. Fuller and V. Cirigliano, *Neutrino Quantum Kinetics*, *Phys. Rev.* **D89** (2014) 105004, [[1309.2628](#)].
- [32] Y. Zhang and A. Burrows, *Transport Equations for Oscillating Neutrinos*, *Phys. Rev.* **D88** (2013) 105009, [[1310.2164](#)].
- [33] V. Cirigliano, G. M. Fuller and A. Vlasenko, *A New Spin on Neutrino Quantum Kinetics*, *Phys. Lett.* **B747** (2015) 27–35, [[1406.5558](#)].
- [34] J. Serreau and C. Volpe, *Neutrino-antineutrino correlations in dense anisotropic media*, *Phys. Rev.* **D90** (2014) 125040, [[1409.3591](#)].
- [35] D. N. Blaschke and V. Cirigliano, *Neutrino Quantum Kinetic Equations: The Collision Term*, *Phys. Rev.* **D94** (2016) 033009, [[1605.09383](#)].
- [36] V. Cirigliano, M. W. Paris and S. Shalgar, *Effect of collisions on neutrino flavor inhomogeneity in the early universe*, [1706.07052](#).
- [37] A. Mirizzi, G. Mangano and N. Saviano, *Self-induced flavor instabilities of a dense neutrino stream in a two-dimensional model*, *Phys. Rev.* **D92** (2015) 021702, [[1503.03485](#)].
- [38] S. Chakraborty, R. S. Hansen, I. Izaguirre and G. Raffelt, *Self-induced flavor conversion of supernova neutrinos on small scales*, *JCAP* **1601** (2016) 028, [[1507.07569](#)].
- [39] A. Mirizzi, *Multi-azimuthal-angle effects in self-induced supernova neutrino flavor conversions without axial symmetry*, *Phys. Rev.* **D88** (2013) 073004, [[1308.1402](#)].
- [40] J. F. Cherry, J. Carlson, A. Friedland, G. M. Fuller and A. Vlasenko, *Neutrino scattering and flavor transformation in supernovae*, *Phys. Rev. Lett.* **108** (2012) 261104, [[1203.1607](#)].
- [41] A. Banerjee, A. Dighe and G. Raffelt, *Linearized flavor-stability analysis of dense neutrino streams*, *Phys. Rev.* **D84** (2011) 053013, [[1107.2308](#)].
- [42] M. T. Keil, G. G. Raffelt and H.-T. Janka, *Monte Carlo study of supernova neutrino spectra formation*, *Astrophys. J.* **590** (2003) 971–991, [[astro-ph/0208035](#)].
- [43] B. Gough, *GNU Scientific Library Reference Manual - Third Edition*. Network Theory Ltd., 3rd ed., 2009.